

Prospects of observation of gravitationally lensed sources by space submillimeter telescopes.

© 2019 T.I. Larchenkova^{1*}, A.A. Ermash¹, A.G. Doroshkevich¹

¹ *Lebedev Physical Institute of Russian Academy of Sciences, Moscow, Russia.*

ABSTRACT

In the current paper we consider the prospects of observation of gravitationally lensed sources in far-infrared and submillimeter wavelength ranges by the future space telescopes equipped with actively cooled main mirrors. We consider the possibility of solving some of the important cosmological and astrophysical scientific tasks by observation of gravitationally lensed sources. The number counts of lensed sources for wavelengths from $70\mu m$ up to $2000\mu m$ were calculated. We discuss the distribution of lensed sources at different redshifts and magnification coefficients and also mass distribution of lenses. Model sky maps that illustrate the contribution of lensed sources were created.

Keywords: far IR, galaxy evolution, gravitational lensing.

* E-mail: ltanya@asc.rssi.ru

INTRODUCTION

Modern astrophysical instruments with their growing angular resolution and sensitivity make it possible to observe more and more sources that underwent strong gravitational lensing. The gravitational lensing occurs when the light from a distant background object is deflected by a massive object - gravitational lens on the line of sight. Any object can act as a gravitational lens, e.g. galaxy or galaxy group. In the case of strong gravitational lensing multiple images of the source can be observed. Angular distance between such images of a lensed objects increases with the lens mass if the impact parameter remains constant. That is why it is easier to detect lensed systems where lens is a high-mass galaxy or a galaxy cluster. The first discovered strongly lensed object was the quasar B0957+561 with two images that was lensed by a massive galaxy (Walsh et al., 1979). The information about the time delay between the images; their fluxes and coordinates makes it possible to recover the mass distribution in the lens and also to estimate the main cosmological parameters.

If an extended source is lensed, e.g. a galaxy, an Einstein-Chwolson ring or a part of it might be observed. If a massive galaxy cluster acts as a lens, galaxies beyond it are observed as bright extended arcs. Such arcs were discovered in the galaxy cluster A370 (Soucail et al., 1987; Lynds, Petrosian, 1986) and interpreted in Paczynski (1987) as images of lensed background galaxies.

The amount of known gravitationally lensed systems is limited. For example, in the CASTLES¹ catalog there are about a hundred of objects with multiple images. Such objects provide crucial information for a number of cosmological and astrophysical tasks.

One of such tasks is the independent determination of the Hubble constant H_0 (see, e.g., Refsdal 1964; Suyu et al. 2017). It is one of the main cosmological parameters that describe the velocity of expansion, age, size and critical density of the Universe. Other cosmological parameters beside the Hubble constant can also be constrained (see, e.g. Blandford, Narayan 1992). Strong gravitationally lensed sources allow us to observe the very high redshift objects due to significant flux magnification. The information of the lenses themselves (galaxies and galaxy clusters) can also be obtained. One can derive dark matter distribution (see, e.g., Kochanek 1991), initial mass function, SMBH evolution and the influence of the AGN feedback (Peng et al., 2006). Some papers are dedicated to the low-mass subhalo detection, see the pioneering work by Mao, Schneider (1998).

Instruments that have sufficient sensitivity and angular resolution make it possible to explore the aforementioned problems in various wavelength ranges, including far-infrared (FIR), submillimeter and millimeter wavelengths. There are several future space observatories with actively cooled main mirrors that will perform observations in this wavelength range, such as SPICA² and OST³, but Millimetron is the only one that is expected to be launched in the next decade (Smirnov et al., 2012; Kardashev et al., 2014; Kardashev, 2017). Millimetron can perform observations dedicated to all of the aforementioned scientific tasks, including Lyman-alpha emitters, first galaxies and high-redshift dusty starforming galaxies (DSFGs) (see review by Casey et al. 2014).

Aside from using gravitational lensing for tasks of astrophysics and cosmology it plays crucial role in modeling of the extragalactic background. The gravitational lensing significantly affects number counts in submillimeter and millimeter wavelengths due to the steepness of the curve (see, e.g., Béthermin et al. 2011; Pilipenko et al. 2017). Observations in these wavelength ranges showed that the number of sources with large fluxes varies for different sky areas. This effect is caused by gravitational lensing of sources on galaxies and galaxy clusters (Aretxaga et al. 2011), see also discussion in Hayward et al. (2013).

In this paper we discuss the possible contribution of the Millimetron mission to these scientific tasks. The structure of the paper is as follows. In section 1 we give the information about the parameters of the Millimetron mission and the description of the model used to estimate the parameters of lensed objects. In section 2 we estimate the number of lensed sources for different wavelengths, their contribution to the number counts, redshift distribution of lensed sources, magnification coefficient distribution and mass distribution. Model maps that illustrate the contribution of lensed sources are also given. In section 3 we consider important astrophysical tasks and the expected parameters of gravitationally lensed systems. In section 4 we describe the obtained results and give a short discussion.

¹www.cfa.harvard.edu/castles

²spica-mission.org

³asd.gsfc.nasa.gov/firs

1. The main parameters of the model and the Millimetron space observatory

The model that was used to perform all calculations in this paper was described in detail in Ermash et al. (2018). We have used the numerical model of the dark matter evolution from Cousin et al. (2015). The simulation contained 1024^3 particles with mass $8.536 \times 10^7 M_\odot$ in volume $\sim 150 \text{ Mpc}^3$. The parameters of the Cosmology were as following. Matter density $\Omega_m = 0.24$, dark energy density $\Omega_\Lambda = 0.76$, baryon fraction $f_b = 0.16$, dimensionless Hubble constant $h = 0.73$. Minimum halo mass was $1.7 \times 10^9 M_\odot$. We created the cone from the simulation following the approach by Blaizot et al. (2005). Each cube was affected by a random transformation: turn by $-\pi/2$, 0 or $+\pi/2$, random shift and mirroring independently on each axis. Such an approach helps to overcome the effect of perspective. Next we create a SED library using the GRASIL code (Silva et al., 1998).

The main difference between the model used in this paper (Ermash et al., 2018) and our previous model published in Pilipenko et al. (2017) is that we used this model SED (Spectral Energy Distribution) library. Each galaxy was assigned a closest in parameter space model SED (age of galaxy, stellar mass, mass of gas, star formation rate, size and metallicity). For each disk and bulge 10 SEDs for different inclination angles was created (0° , 10° etc). Inclination angle of each galaxy was chosen randomly. We utilized the AGN SED from Lyu, Rieke (2017).

Each object of the simulation was assigned a SED according to its physical parameters. Then we calculated the number counts, created model maps for various wavelengths etc.

Model maps and number counts are significantly affected by the effect of lensing of distant objects. It becomes more apparent on larger wavelengths. Earlier Negrello et al. (2010); Béthermin et al. (2011); Pilipenko et al. (2017) showed that the expected fraction of lensed sources at $500\mu m$ with flux greater than 100 mJy is about 15% and reaches 40% at $1000\mu m$. Two simple models of a gravitational lens were considered in this paper: point lens and singular isothermic sphere (see, e.g. Schneider et al. 1992). Only events with magnification greater than or equal to 2 will be considered in this paper.

The main parameters of the Millimetron observatory are given in Smirnov et al. (2012); Kardashev et al. (2014); Kardashev (2017) and on the official web-site of the project⁴. It will have an actively cooled to 10K main mirror. Photometric observations will be performed by the Long wave Array Camera Spectrometer (LACS) and Short wave Array Camera Spectrometer (SACS). List of the wavelength bands and the corresponding FWHMs are given in table 1. At $\lambda > 300\mu m$ angular resolution is limited by diffraction, and at the shortest band it will be about 1-2 angular seconds. The expected sensitivity of the wide band photometry is about 0.01 mJy . The field of view of the telescope is $6' \times 6'$.

2. Model maps and lensed source counts

In order to approach scientific tasks connected with gravitationally lensed systems photometric and spectroscopic observations are required. The goal of photometric observations

⁴millimetron.ru

Table 1: Parameters of the LACS and SACS detectors of the Millimetron observatory

Wavelength (μm)	FWHM (")	
Long wave Array Camera Spectrometer (LACS)		
Band 1	3000–1500	42
Band 2	1500–850	22
Band 3	850–450	12
Band 4	450–300	7.5
Short wave Array Camera Spectrometer (SACS)		
Band 1	50–90	1–2
Band 2	90–160	2–4
Band 3	160–300	4–6
Band 4	300–450	6–10

Table 2: Confusion limit estimations for the Millimetron mission.

Wavelength (μm)	Source density criterion (mJy)	Photometry criterion $q = 5$ (mJy)	Probability of deflection $P(D) \ 5\sigma$ (mJy)
70	1.8×10^{-3}	6×10^{-4}	1.9×10^{-3}
110	3.50×10^{-2}	3.6×10^{-3}	2.57×10^{-2}
250	2.19	1.44×10^{-1}	2.18
350	2.91	3.90	3.99
650	1.62	3.44	3.37
850	1.01	2.41	2.34
1100	6.06×10^{-1}	1.59	1.51
2000	1.66×10^{-1}	4.63×10^{-1}	4.30×10^{-1}

is the detection of galaxies and AGN on observational maps and study of their physical properties and evolution. The number counts is a widely used statistical description of the observed sources. They can be represented in integral $N(> S)[\text{deg}^{-2}]$ or differential $dN/dS[\text{mJy}^{-1}\text{deg}^{-2}]$ form. The number counts can be used to derive the background intensity and to make some estimates of the confusion noise. This effect takes place when there are more than one source per beam. Far infrared and submillimeter observations are significantly affected because of the limited angular resolution. The confusion limit for the Millimetron mission is shown in table 2 for a list of wavelengths. Our estimations show that, e.g. at $110\mu m$ confusion is $\sim 10^{-2}$ mJy, that is significantly better than the confusion limit of the Hershel observatory.

As was shown earlier (see, e.g., Béthermin et al. 2011; Pilipenko et al. 2017; Ermash et al. 2018) gravitational lensing significantly changes the shape of the number counts curve. This effect is most prominent at millimeter and submillimeter wavelengths at fluxes larger than ≥ 100 mJy. This effect can be seen on fig. 1. The upper panel shows differential number counts of the BM (Béthermin et al., 2011) and P2017 (Pilipenko et al., 2017) models, central panel shows steepness of the curve for the BM model, lower panel – change in number counts due to the lensing effect.

2.1. Gravitationally lensed sources on model maps

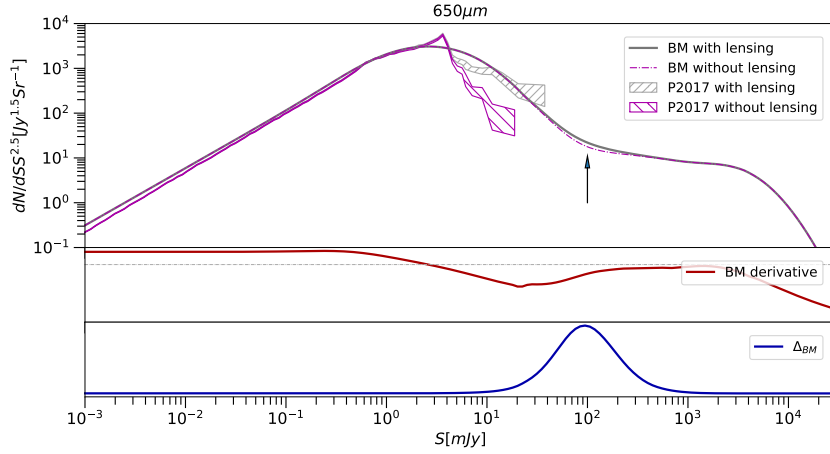


Figure 1: Upper panel - differential number counts at $650\mu m$ of the BM and P2017 models with and without lensing, middle panel – steepness of the number counts curve, lower panel – change of the number counts due to the lensing.

In order to demonstrate the prospects of observation of lensed sources with the Millimetron mission we plot model maps of a small area for eight wavelengths from 70 to $2000\mu m$ (see figs 2 and 3). The area of model maps is the same as the field of view of Millimetron.

In the process of creating the maps we accepted the following simplifications: sources were considered as point sources, the beam of the instrument was Gaussian. Intensity is in logarithmic scale. Pixel angular size increases with wavelength. So, for example, pixel size is $0.6''$ for $70\mu m$, $0.9''$ for $110\mu m$, $2''$ for $250\mu m$, $2.8''$ for $350\mu m$, $4''$ for $500\mu m$.

In order to visualize the contribution of lensed sources we used the following approach. Let us consider a pixel that has a flux in RGB channels R_{old} , G_{old} and B_{old} . If we have to add to this pixel the flux S_ν of an unlensed source, we add it the following way:

$$\begin{aligned} R_{new} &= R_{old} + S_\nu, \\ G_{new} &= G_{old} + S_\nu, \\ B_{new} &= B_{old} + S_\nu \end{aligned}$$

The flux of a lensed source with magnification μ_{obj}^* is added the following way:

$$\begin{aligned} R_{new} &= R_{old} + S_\nu \times \\ &(1 + (\mu_{obj} - \mu_{min})/(\mu_{max} - \mu_{min}) * 2), \\ G_{new} &= G_{old} + S_\nu \times \\ &(1 - (\mu_{obj} - \mu_{min})/(\mu_{max} - \mu_{min})), \\ B_{new} &= B_{old} + S_\nu \times \\ &(1 - (\mu_{obj} - \mu_{min})/(\mu_{max} - \mu_{min})), \end{aligned}$$

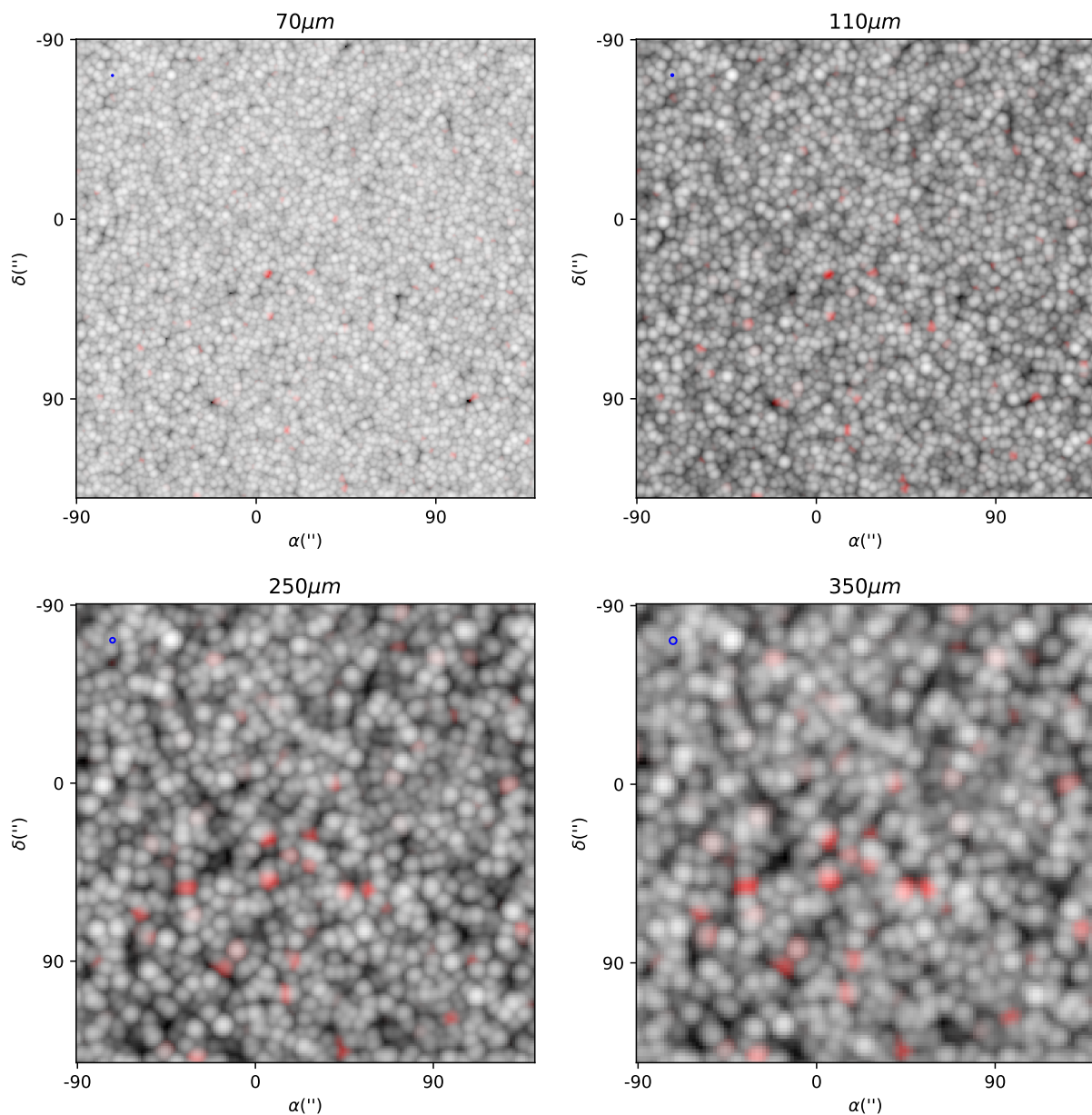


Figure 2: Model maps of the $3' \times 3'$ area for 70, 110, 250 and 350 μm . Angular resolution corresponds to the diffraction limit of a 10m mirror, pixel size is FWHM/3. Blue circle at the top left of every map shows the beam size. Lensed sources with magnification ≥ 2 are depicted as red. Detailed description see in text.

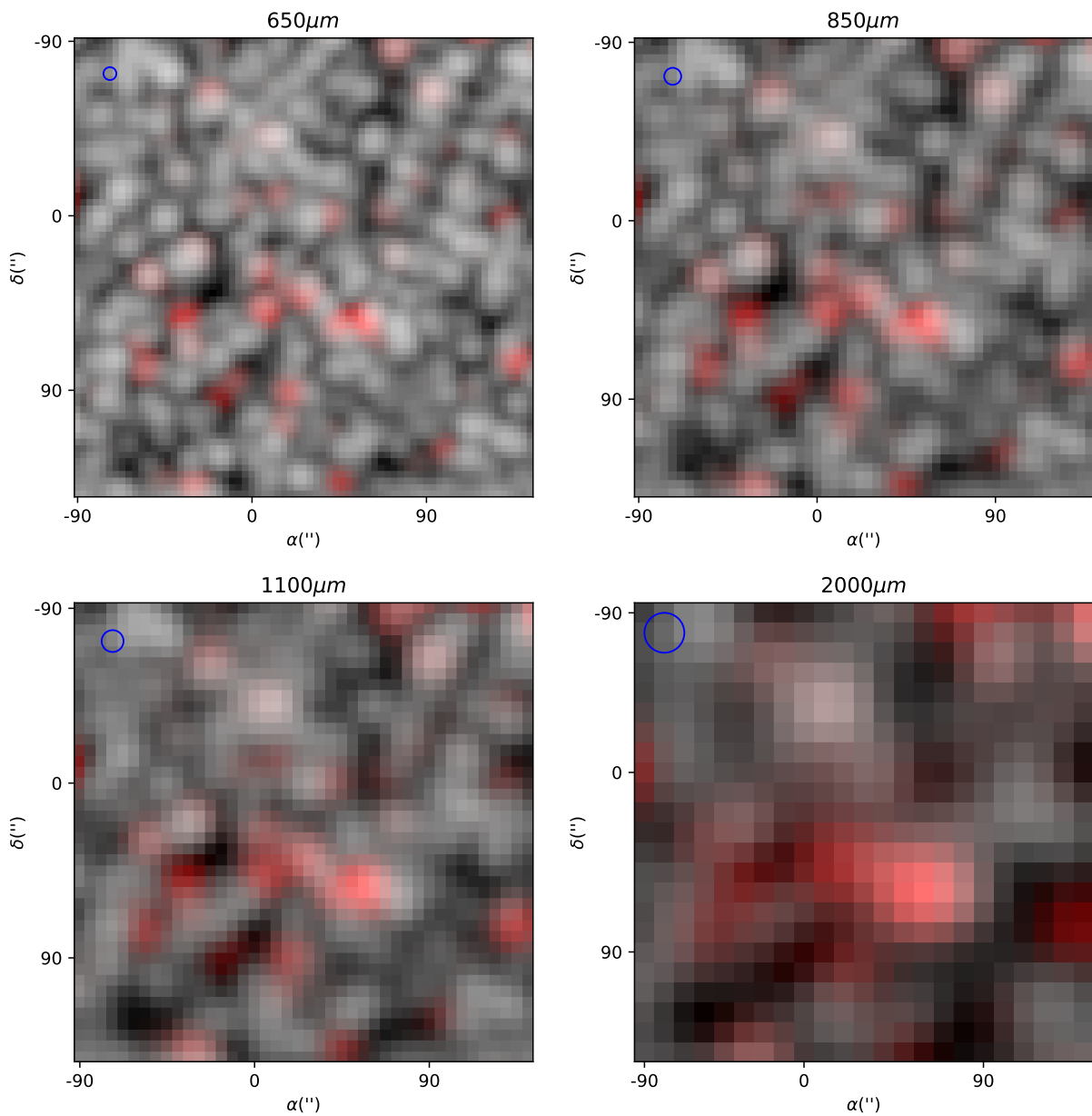


Figure 3: Model maps for 650, 850, 1100 and 2000 μm . Details are the same as on fig. 2.

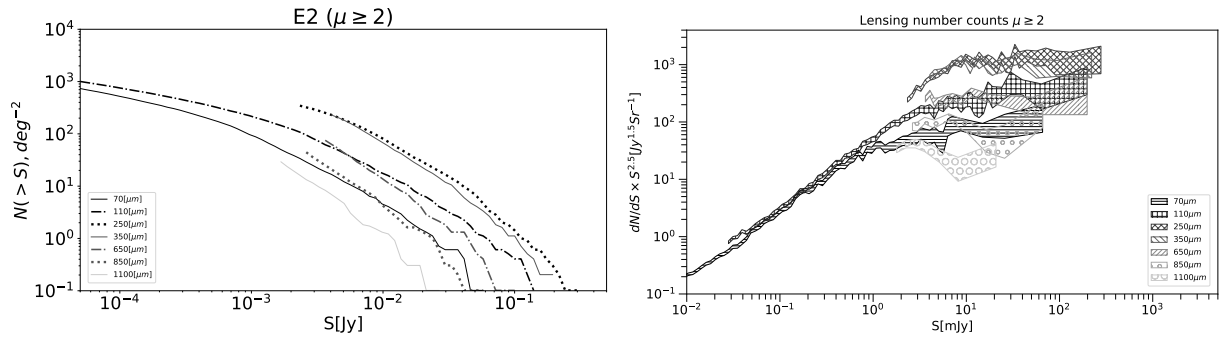


Figure 4: Number counts of sources with magnification coefficient $\mu \geq 2$ for the following wavelengths: 70, 110, 250, 350, 650, 850, 1100 μm . Left – integral number counts $N(S)$; right - differential number counts.

where $\mu_{obj} = \min(\mu_{obj}^*, \mu_{max})$, μ_{min} – is the minimum value of the lensing coefficient, μ_{max} – the maximum value.

It is obvious that for an unlensed source the magnification coefficient is equal to 1. Let us consider it as a minimal possible value μ_{min} . In case of a point source magnification can sometimes reach very high values. But real sources have finite angular size that limits maximum lensing magnification and the probability of precise alignment of source and lens is quite low. As will be shown in the following text the amount of sources with magnification greater than 2–3 is relatively low. That is why in model maps μ_{max} was set to 3 in order to highlight most of the lensed sources, not only strongly lensed ones.

From the model maps on figs 2 and 3 it can be clearly seen that with increase of wavelength the contribution of lensed sources increases while angular resolution decreases. This effect can be explained by the growing contribution of distant sources. It was already noted in numerous papers, see, e.g. Negrello et al. (2007, 2010); Béthermin et al. (2011) and references therein. The reason behind it is the negative K-correction which means that for wide range of redshifts $z \approx 1 - 4$ flux does not depend on redshift.

2.2. Number counts of gravitationally lensed sources

In order to approach the aforementioned scientific tasks and to create a draft of the observational program it is necessary to estimate the amount of lensed systems available for observation on different wavelengths. We built integral and differential number counts of lensed sources with $\mu \geq 2$ that are shown on fig. 4. For example, the amount of sources with $\mu \geq 2$ and flux greater than $\geq 1mJy$ is ~ 1000 at millimeter and submillimeter wavelengths.

In order to estimate the amount of potentially observable lensed sources with $\mu \geq 2$ on various redshifts, even at $z \geq 2$, we need to know their exact redshift distribution. Such distribution is shown on figure 5 on the upper panel. The number of lensed sources grows up to $z \sim 1.5$ on all wavelengths. At higher redshifts on far infrared wavelengths it decreases rapidly with redshift, while on submillimeter wavelengths more gradual decline can be seen due to the negative K-correction.

The normalized distribution of lensed sources with $\mu \geq 2$ by the lensing coefficient is shown on the central panel of figure 5. From this distribution it can be clearly seen that most of the lensed sources have magnification coefficients between 2 and 5. This is in agreement with the results of Hershel observatory that bright lensed sources with $S_{500\mu m} > 100\text{mJy}$ have average magnification coefficient $\mu \approx 6_{-3}^{+5}$ (Bussmann et al., 2013).

In order to estimate the expected typical angular distance between lensed images of the object we need the information about the mass distribution of the lenses. This distribution is shown on the lower panel of figure 5. It can be seen that maximum of the distribution is about $10^{11}M_{\odot}$. For a lens with such a mass angular distance between images will be about one angular second and that is comparable with the Millimetron angular resolution (see table 1). It is important to note that lensed DSFG galaxies that were detected on the SPT (South Pole Telescope) and were targets of follow up high resolution ALMA observations had angular separation between lensed images about $\sim 1\text{-}2$ angular seconds (see, e.g., Hezaveh et al. 2013). That value is in agreement with the maximum of the mass distribution of lenses. The predicted mass distribution leads to the conclusion that half of lensed sources will have angular separation of images larger than 1 angular second.

3. Scientific tasks and prospects of their solving

Let us now consider most actual scientific tasks that can benefit from observations in far IR, submillimeter and millimeter wavelengths.

3.1. Independent determination of the Hubble constant

As was already discussed above, the determination of the Hubble constant is one of the important scientific task because this constant defines modern expansion rate of the Universe, its age, size and critical density. Now there is a discrepancy at 4.4σ level between the value obtained by the Hubble Space Telescope with the "distance ladder" (Riess et al., 2019) ($H_0 = 74.03 \pm 1.42(\text{km/s})/\text{Mpc}$) and the value obtained by the Planck mission in ΛCDM model by the measurements of the CMB (Planck Collaboration et al., 2018) ($H_0 = 67.4 \pm 0.5(\text{km/s})/\text{Mpc}$). Data obtained from analysis of baryonic acoustic oscillations together with data on first type supernova (SNe Ia) give a result close the value obtained by Planck observatory $H_0 = 67.3 \pm 1.0 (\text{km/s})/\text{Mpc}$ (Alam et al., 2017).

The H_0 value derived from megamaser observations $H_0 = 66.0 \pm 6.0 (\text{km/s})/\text{Mpc}$ (Gao et al., 2016) and in the Carnegie-Chicago Hubble Program $H_0 = 69.8 \pm 0.8(\pm 1.1\%stat) \pm 1.7(\pm 2.4\%sys) (\text{km/s})/\text{Mpc}$ (Freedman et al., 2019) are also close to this value.

So the results of recent observations show signs that for local Universe and the distant Universe the value of the Hubble constant might differ. If that is really the case, then the ΛCDM model should be modified. E.g. one should consider dynamical dark matter, non-zero curvature, larger number of effective relativistic particles etc. In order to figure out the nature of the discrepancy of H_0 independent methods of its measurement should be used. One of such methods is the measurement of the so-called delay distance between multiple

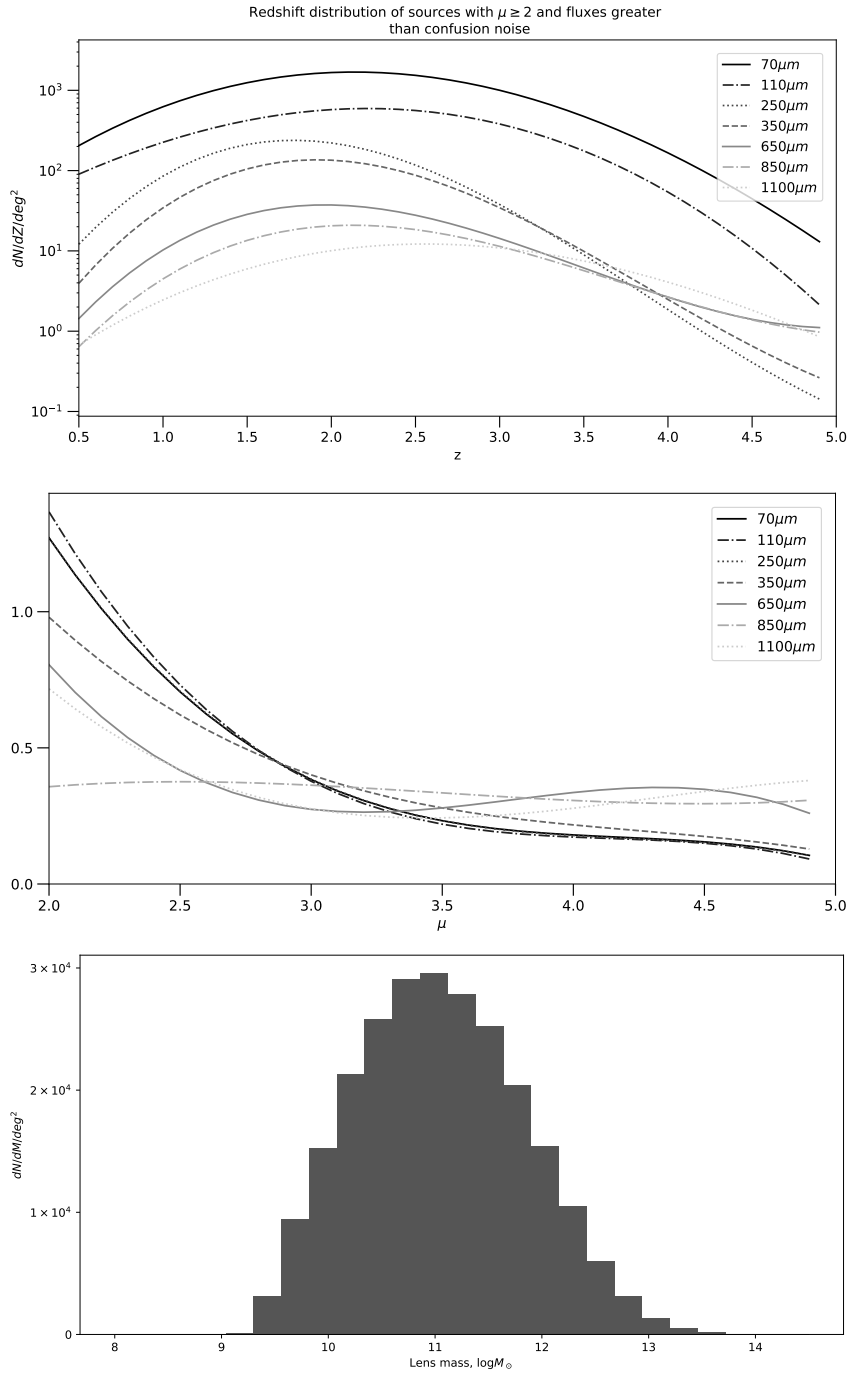


Figure 5: Upper panel – redshift distribution of gravitationally lensed sources with magnification coefficient greater than $\mu \geq 2$ for the following wavelengths: 70, 110, 250, 350, 650, 850, 1100 μm . Central panel – magnification coefficient distribution of sources (normalized). Lower panel – mass distribution of lenses with $\mu \geq 2$.

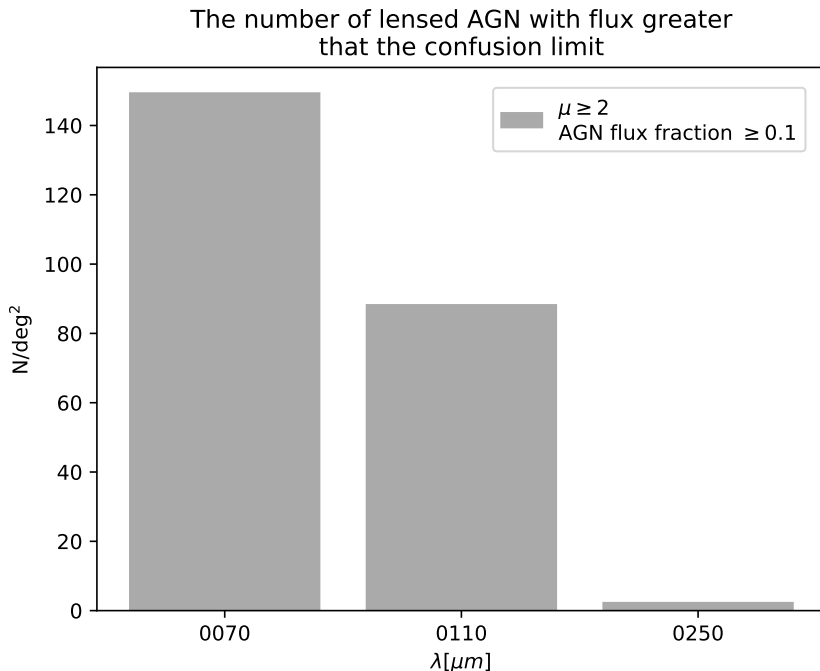


Figure 6: The histogram showing the number of lensed AGN on 70–250 μm with flux greater than the confusion limit and the lensing coefficient $\mu \geq 2$.

images of a bright variable lensed source, like quasar or a supernova. This approach was developed by Refsdal (1964). The delay distance is reversely proportional to the value of the Hubble constant. Such an approach can be used not only to constraint the value of this constant but also another cosmological parameters. The delay distance is determined by the measurement of delay of photons from different images of the lensed source. But the delay itself is not sufficient to determine the H_0 with good enough accuracy (see, e.g., Larchenkova et al. 2011). Suyu et al. (2014) showed that for one lensed object with measured time delay and some additional observational data the Hubble constant can be derived with 7–8% accuracy. Today the Hubble constant is measured with 2.4% accuracy by the analysis of six lensed quasars and is found to be $73.3^{+1.7}_{-1.8}$ (km/s)/Mpc (Wong et al., 2019). So, taking this result into account, the tension between the estimations, the discrepancy between estimations of the H_0 by the analysis of observational data of young and local Universes is 5.3σ . But in order to solve the problem of the discrepancy between the estimations of the Hubble constant from various experiments and to obtain the information about the dark energy the 1% accuracy is required. For such accuracy one needs to have detailed information and the time delay between images for about 40 gravitationally lensed systems (see, e.g. Wong et al. 2019 and references therein).

All the aforementioned estimations of the Hubble constant were obtained by means of observation in the visible, near infrared or radio wavelength ranges. The Millimetron space telescope will be able to provide additional information about gravitationally lensed systems in far infrared and submillimeter wavelength ranges. According to the table 1 the resolution of the telescope at the shortest wavelengths will be about 1–2 angular seconds and the sensitivity of the wideband photometry will reach 0.01 mJy.

In order to estimate the number of potentially observable gravitationally lensed systems that can be used for the estimation of H_0 we need to know the amount of AGN with magnification coefficient $\mu \geq 2$ and the distribution of masses of lenses to estimate the angular distance between images. The number of quasars with $\mu \geq 2$ at $70\text{--}250\mu m$ with flux greater than the confusion limit is shown on fig. 6. This histogram is created for the objects with the AGN flux fraction greater than 0.1. It can be seen that about 140 AGN with $\mu \geq 2$ can be detected on the sky area of one square degree in the wavelength range $70\text{--}250\mu m$. The histogram of the distribution of the masses of lenses is shown on figure 5. From this distribution a conclusion can be made that about a half of lensed sources will have angular separation of images greater than one angular second and about $\sim 15\%$ greater than 2 angular seconds.

According to these estimates in order to register 40 lensed AGNs with angular separation between images greater than 2 angular seconds the survey of 2 square degree area is required. The scan speed of the Millimetron space telescope will be about 0.005 sq. deg. per minute, so the observation time required is about 7 hours.

Another promising approach for the task considered is to observe previously detected AGNs in different wavelengths that have measurements of time delay between images of a variable source. Observations of AGN in far infrared wavelength range will provide additional information that together with data at other wavelength ranges will make the independent estimation of the Hubble constant with required accuracy possible in order to determine the difference between this value in the local and distant Universes. It must be stressed that for this task, like for all other scientific tasks dedicated to the study of gravitationally lensed sources, besides the photometric observations with high sensitivity and fine angular resolution spectroscopic data with high spectral resolution are required in order to derive spectroscopic redshifts of lenses and lensed sources.

3.2. Distant galaxies with high amount of dust and active star formation

Dusty Star Forming Galaxies are most massive and have extreme star formation rates, their typical stellar mass and SFR are $\sim 10^{10}M_\odot$ and $\sim 100M_\odot\text{yr}^{-1}$, respectively (see, e.g., review by Casey et al. 2014 and references therein). Due to such extreme star formation these galaxies host large amounts of dust. More than 95% of the radiation comes from hot young stars surrounded by dust that re-emits the UV radiation in far IR (see, e.g. Sanders, Mirabel 1996; Blain et al. 2002).

In the local Universe such galaxies are quite rare, while at $z \sim 2$ they are about 1000 times more frequent and become the main contributors to the total star formation in the Universe (see, e.g. Casey et al., 2014, and references therein). Probably all the DSFG are the result of merging of galaxies or are massive gas rich disc galaxies in stage of intense star formation (see, e.g. Ivison et al. 2012; Hodge et al. 2016).

On high redshifts ($z > 2.5$) the volume density of DSFG is unknown. The same can be said about their contribution to the global star formation rate in the Universe. The knowledge about the properties of DSFG in early Universe is crucial for understanding

of the mechanisms of galaxy formation and star formation processes in early Universe and formation of dust (supernova, AGB stars or growth of dust particles in interstellar medium).

Today there are 77 discovered candidates in bright DSFG in HerMES Large Mode Survey and Hershel Stripe 82 Survey that covers 372 sq. degrees (Nayyeri et al., 2016). List of about a hundred of potential candidates can be found in Vieira et al. (2013).

As was mentioned above, the best strategy to search for submillimeter lensed galaxies on high redshifts is to perform wide area shallow surveys due to the negative K-correction.

The expected amount of lensed galaxies with $\mu \geq 2$ on a 1 square degree area is expected to be 10^2 – 10^3 for different wavelengths (see number counts curves on fig. 4). Because of the high sensitivity the scan speed will reach 0.05 square degrees per minute at $\lambda > 110\mu m$ and an order of magnitude lower at shorter wavelengths. The area of one square degree can be covered by Millimetron in ~ 20 or ~ 200 minutes depending on the exact wavelength. According to the aforementioned estimations 90% of the strongly lensed objects will be distant DSFG. Final determination of the object’s type will require the SED analysis. The most promising strategy to enlarge the sample of DSFGs with $z \sim 1 - 2$ and to search for weak distant sources is the observation of galaxy clusters in far infrared and submillimeter wavelengths (see, e.g. Zemcov et al. 2013). Galaxy clusters are mainly populated by early type galaxies that do not have significant emission in submillimeter wavelengths, so clusters are in fact act as transparent lenses. Galaxy clusters from “The Heshel Lensing Survey” and “HST Frontier Field Coverage” will be included in the observation program. These fields will be scanned two orders of magnitude faster compared to the Hershel obsevatory. Moreover, many of these clusters have the known distribution of gravitational potential, accurate mass and distance measurements, in another words one have accurate model of the lens.

3.3. *First galaxies*

Another important task for cosmology is the study of the earliest galaxies that probably played the key role in the reionization of the Universe and in the radiation heating at high redshifts $z \approx 7 - 12$ (see, e.g. Kakiichi et al. 2016). Such heating prevents the accretion of baryons onto low mass haloes that causes the decrease of amount of low mass haloes containing stars. The heating of interstellar medium suppresses the star formation in massive haloes, in another words leading to the decrease of star formation rate. It is expected that masses, luminosities and metallicities in early galaxies were close to the values for the satellites of our Galaxy and Andromeda galaxy. The researches of the dwarf galaxies of Local Group showed that formation of metals is possible after the formation of the galaxy or in the later period (Weisz et al., 2014). In order to find out which scenario took place in the first galaxies it is necessary to observe high redshift galaxies.

It is possible that the so-called Lyman-Alpha Emitters (LAE) are connected to the first galaxies. These are extremely bright objects that emit significant portion of their energy in the $L\alpha$ line due to the scattering of the UV radiation of the central source

(or the star formation region) in the surrounding envelope consisting of neutral or mildly ionized hydrogen. These objects are distributed in a wide range of redshifts up to $z \sim 11$, which points to the fact that they play a crucial role in the reionization of the Universe. Observations of several hundreds of LAE candidates lead to the conclusion that they are low mass galaxies with active star formation and that they can be considered as progenitors of dwarf galaxies in local group (see, e.g. Hao et al. 2018; Shibuya et al. 2018).

LAE on high redshifts will be observed in the Paschen and Brackett series that fall in the wavelength range of the Millimetron telescope. Despite the fact that their intensity is low, the sensitivity of the Millimetron detections ($\sim 10^{-22} W m^2$) will make their detection possible. The magnification of these objects due to gravitational lensing makes their detection more likely.

The preferred targets for registration of LAE’s emission are massive galaxy clusters that are listed in Coe et al. (2019). To solve one of the key task the Millimetron scientific program will include observation of about a hundred of such clusters. Considering the results obtained by Coe et al. (2019) we expect to detect several hundred of LAE candidates. The selected candidates will become targets of spectroscopic observations in submillimeter and millimeter wavelength ranges. The lines of interes are [CII] 158 μm , [OIII] 88 μm , [OI] 63 μm and CO lines.

In the recent years there was a significant progress in the spectroscopy of the lensed galaxies, including galaxies lensed on galaxy clusters (see, for example, Stark et al., 2014, 2015). Recently Kanekar et al. 2013; Laporte et al. 2019; Matthee et al. 2019 showed that lensed LAE do not show [CII] emission that is clearly observed in the submillimeter galaxies.

The Millimetron observatory will increase the LAE sample and analyze the emission in this line with high sensitivity and resolution. That will allow to validate the hypothesis of existence of several kinds of LAE galaxies.

3.4. Another scientific tasks

It is a well known fact that numerical simulations following the standard Λ CDM model reproduce the large-scale structure fairly well, but the amount of observed galaxies is significantly lower that modeled. This is the definition of the so-called satellite problem. That is why the knowledge about the exact number of low mass galaxies is crucial for the choice of the cosmological model and the dark matter model. The strong gravitational lensing gives the most straight approach of determination of the dark matter distribution on sub-galactic scale. Mao, Schneider (1998) proposed to use the observed ratio of fluxes of lensed images of quasars to limit the number of massive structures (subhalo) in galaxies that work as lenses. Dalal, Kochanek (2002) used relatively small sample of seven lensed quasars to derive statistical limitations on the amount of the projected mass contained in substructures. They showed that in general it corresponds to the results of numerical simulations in the Λ CDM model. The same problem was also considered in Metcalf, Zhao (2002). At the same time another analysis by Xu et al. (2009, 2015) showed that the

population of substructures predicted by numerical methods is insufficient to explain the observed anomalies in the ratio of fluxes of lensed images. These anomalies can be probably explained by the presence of complex baryonic structures in lensing galaxies and also by a presence of dark subhaloes on the line of sight.

Aside from the analysis of anomalous flux ratios of lensed images there are other methods to detect substructures in strongly lensed sources. One of such approaches is the "gravitational imaging" technique that uses the extended arcs and Einstein rings to detect and analyze the masses of separate subhaloes (see, for example, Koopmans, 2005; Vegetti, Koopmans, 2009). This approach considers the substructures not as analytical clumps of mass but instead as linear pixel corrections of global lensing potential. That is why it does not require any assumptions on the number of substructures and their density profile and redshift. To say more, this approach can easily discriminate between the presence of a substructure and smooth but complex mass distribution. That is why this method is less prone to false detections. But in contrast to the analysis of anomalous flux ratios in order to detect a low-mass subhalo observational data with high resolution and high flux dynamic range are required.

4. Discussion

In this paper we have discussed the prospects of observation of gravitationally lensed extragalactic sources in far infrared and submillimeter wavelength ranges by the next scheduled for launch space observatory with actively cooled main mirror that will perform observations in this wavelength range. All the calculations were performed accordingly to the declared specifications of the observatory, in particular the cooled ($T < 10\text{K}$) main 10m mirror with high sensitivity detectors that will work in wavelength range $70 - 2000 \mu\text{m}$. The number counts of lensed sources for different wavelengths were calculated. We built the distributions of the lensed sources by redshift and magnification coefficient and the mass distribution of lenses. We created model sky maps that illustrate the contribution of lensed sources. The prospects to solve actual cosmological and astrophysical tasks connected to the observation of gravitationally lensed systems were discussed. Among them are the research of distant galaxies with active star formation and significant amount of dust (DSFG), first galaxies such as Lyman-Alpha emitters, independent determination of Hubble constant and other cosmological parameters (e.g. dark energy), subhalo detection, dark matter distribution in galaxies and massive galaxy clusters.

This study was supported by the program KP19-270 "Questions of origin and evolution of the Universe with ground based and space researches."

Bibliography

- Alam S., Ata M., Bailey S., Beutler F., Bizyaev D., Blazek J. A., Bolton A. S., Brownstein J. R., Burden A., Chuang C.-H., Comparat J., Cuesta A. J., Dawson K. S., Eisenstein D. J., Escoffier S., Gil-Marín H., Grieb J. N., Hand N., Ho S., Kinemuchi K., Kirkby D., Kitaura F., Malanushenko E., Malanushenko V., Maraston C., McBride C. K., Nichol R. C., Olmstead M. D., Oravetz D., Padmanabhan N., Palanque-Delabrouille N., Pan K., Pellejero-Ibanez M., Percival W. J., Petitjean P., Prada F., Price-Whelan A. M., Reid B. A., Rodríguez-Torres S. A., Roe N. A., Ross A. J., Ross N. P., Rossi G., Rubiño-Martín J. A., Saito S., Salazar-Albornoz S., Samushia L., Sánchez A. G., Satpathy S., Schlegel D. J., Schneider D. P., Scóccola C. G., Seo H.-J., Sheldon E. S., Simmons A., Slosar A., Strauss M. A., Swanson M. E. C., Thomas D., Tinker J. L., Tojeiro R., Magaña M. V., Vazquez J. A., Verde L., Wake D. A., Wang Y., Weinberg D. H., White M., Wood-Vasey W. M., Yèche C., Zehavi I., Zhai Z., Zhao G.-B.* The clustering of galaxies in the completed SDSS-III Baryon Oscillation Spectroscopic Survey: cosmological analysis of the DR12 galaxy sample // *Mon. Not. Roy. Astron. Soc.* IX 2017. 470. 2617–2652.
- Aretxaga I., Wilson G. W., Aguilar E., Alberts S., Scott K. S., Scoville N., Yun M. S., Austermann J., Downes T. P., Ezawa H., Hatsukade B., Hughes D. H., Kawabe R., Kohno K., Oshima T., Perera T. A., Tamura Y., Zeballos M.* AzTEC millimetre survey of the COSMOS field - III. Source catalogue over 0.72 deg^2 and plausible boosting by large-scale structure // *Mon. Not. Roy. Astron. Soc.* VIII 2011. 415. 3831–3850.
- Béthermin M., Dole H., Lagache G., Le Borgne D., Penin A.* Modeling the evolution of infrared galaxies: a parametric backward evolution model // *Astron. Astrophys.* V 2011. 529. A4.
- Blain A. W., Smail I., Ivison R. J., Kneib J.-P., Frayer D. T.* Submillimeter galaxies // *Phys. Rep.* X 2002. 369. 111–176.
- Blaizot J., Wadadekar Y., Guiderdoni B., Colombi S. T., Bertin E., Bouchet F. R., Devriendt J. E. G., Hatton S.* MoMaF: the Mock Map Facility // *Mon. Not. Roy. Astron. Soc.* VI 2005. 360. 159–175.
- Blandford R. D., Narayan R.* Cosmological applications of gravitational lensing // *Ann. Rev. Astron. Astrophys.* 1992. 30. 311–358.
- Bussmann R. S., Pérez-Fournon I., Amber S., Calanog J., Gurwell M. A., Dannerbauer H., De Bernardis F., Fu H., Harris A. I., Krips M., Lapi A., Maiolino R., Omont A., Riechers D., Wardlow J., Baker A. J., Birkinshaw M., Bock J., Bourne N., Clements D. L., Cooray A., De Zotti G., Dunne L., Dye S., Eales S., Farrah D., Gavazzi R., González Nuevo J., Hopwood R., Ibar E., Ivison R. J., Laporte N., Maddox S., Martínez-Navajas P., Michalowski M., Negrello M., Oliver S. J., Roseboom I. G., Scott D., Serjeant S., Smith A. J., Smith M., Streblyanska A., Valiante E., van der Werf P., Verma*

- A., Vieira J. D., Wang L., Wilner D.* Gravitational Lens Models Based on Submillimeter Array Imaging of Herschel-selected Strongly Lensed Sub-millimeter Galaxies at $z > 1.5$ // *Astrophys. J.*. XII 2013. 779. 25.
- Casey C. M., Narayanan D., Cooray A.* Dusty star-forming galaxies at high redshift // *Phys. Rep.*. VIII 2014. 541. 45–161.
- Coe D., Salmon B., Bradac M., Bradley L. D., Sharon K., Zitrin A., Acebron A., Cerny C., Cibirka N., Strait V., Paterno-Mahler R., Mahler G., Avila R. J., Ogaz S., Huang K.-H., Pelliccia D., Stark D. P., Mainali R., Oesch P. A., Trenti M., Carrasco D., Dawson W. A., Rodney S. A., Strolger L.-G., Riess A. G., Jones C., Frye B. L., Czakon N. G., Umetsu K., Vulcani B., Graur O., Jha S. W., Graham M. L., Molino A., Nonino M., Hjorth J., Selsing J., Christensen L., Kikuchihara S., Ouchi M., Oguri M., Welch B., Lemaux B. C., Andrade-Santos F., Hoag A. T., Johnson T. L., Peterson A., Past M., Fox C., Agulli I., Livermore R., Ryan R. E., Lam D., Sendra-Server I., Toft S., Lovisari L., Su Y.* RELICS: Reionization Lensing Cluster Survey // *arXiv e-prints*. III 2019. 1903.02002.
- Cousin M., Lagache G., Bethermin M., Blaizot J., Guiderdoni B.* Galaxy stellar mass assembly: the difficulty matching observations and semi-analytical predictions // *Astron. Astrophys.*. III 2015. 575. A32.
- Dalal N., Kochanek C. S.* Direct Detection of Cold Dark Matter Substructure // *Astrophys. J.*. VI 2002. 572. 25–33.
- Ermash A. A., Pilipenko S. V., Lukash V. N.* Modelling Cosmic Infrared Background with evolving galaxies // *arXiv e-prints*. XII 2018. 1812.08575.
- Freedman W. L., Madore B. F., Hatt D., Hoyt T. J., Jang I. S., Beaton R. L., Burns C. R., Lee M. G., Monson A. J., Neeley J. R., Phillips M. M., Rich J. A., Seibert M.* The Carnegie-Chicago Hubble Program. VIII. An Independent Determination of the Hubble Constant Based on the Tip of the Red Giant Branch // *Astrophys. J.*. IX 2019. 882. 34.
- Gao F., Braatz J. A., Reid M. J., Lo K. Y., Condon J. J., Henkel C., Kuo C. Y., Impellizzeri C. M. V., Pesce D. W., Zhao W.* The Megamaser Cosmology Project. VIII. A Geometric Distance to NGC 5765b // *Astrophys. J.*. II 2016. 817. 128.
- Hao C.-N., Huang J.-S., Xia X., Zheng X., Jiang C., Li C.* A Deep Ly α Survey in ECDF-S and COSMOS. I. General Properties of Ly α Emitters at $z \sim 2$ // *Astrophys. J.*. IX 2018. 864. 145.
- Hayward C. C., Narayanan D., Kereš D., Jonsson P., Hopkins P. F., Cox T. J., Hernquist L.* Submillimetre galaxies in a hierarchical universe: number counts, redshift distribution and implications for the IMF // *Mon. Not. Roy. Astron. Soc.*. I 2013. 428. 2529–2547.
- Hezaveh Y. D., Marrone D. P., Fassnacht C. D., Spilker J. S., Vieira J. D., Aguirre J. E., Aird K. A., Aravena M., Ashby M. L. N., Bayliss M., Benson B. A., Bleem L. E.,*

- Bothwell M., Brodwin M., Carlstrom J. E., Chang C. L., Chapman S. C., Crawford T. M., Crites A. T., De Breuck C., de Haan T., Dobbs M. A., Fomalont E. B., George E. M., Gladders M. D., Gonzalez A. H., Greve T. R., Halverson N. W., High F. W., Holder G. P., Holzzapfel W. L., Hoover S., Hrubes J. D., Husband K., Hunter T. R., Keisler R., Lee A. T., Leitch E. M., Lueker M., Luong-Van D., Malkan M., McIntyre V., McMahan J. J., Mehl J., Menten K. M., Meyer S. S., Mocanu L. M., Murphy E. J., Natoli T., Padin S., Plagge T., Reichardt C. L., Rest A., Ruel J., Ruhl J. E., Sharon K., Schaffer K. K., Shaw L., Shirokoff E., Stalder B., Staniszewski Z., Stark A. A., Story K., Vanderlinde K., Weiß A., Welikala N., Williamson R.* ALMA Observations of SPT-discovered, Strongly Lensed, Dusty, Star-forming Galaxies // *Astrophys. J.* IV 2013. 767. 132.
- Hodge J. A., Swinbank A. M., Simpson J. M., Smail I., Walter F., Alexander D. M., Bertoldi F., Biggs A. D., Brandt W. N., Chapman S. C., Chen C. C., Coppin K. E. K., Cox P., Dannerbauer H., Edge A. C., Greve T. R., Ivison R. J., Karim A., Knudsen K. K., Menten K. M., Rix H.-W., Schinnerer E., Wardlow J. L., Weiss A., van der Werf P.* Kiloparsec-scale Dust Disks in High-redshift Luminous Submillimeter Galaxies // *Astrophys. J.* XII 2016. 833. 103.
- Ivison R. J., Smail I., Amblard A., Arumugam V., De Breuck C., Emonets B. H. C., Feain I., Greve T. R., Haas M., Ibar E., Jarvis M. J., Kovács A., Lehnert M. D., Nesvadba N. P. H., Röttgering H. J. A., Seymour N., Wylezalek D.* Gas-rich mergers and feedback are ubiquitous amongst starbursting radio galaxies, as revealed by the VLA, IRAM PdBI and Herschel // *Mon. Not. Roy. Astron. Soc.* IX 2012. 425. 1320–1331.
- Kakiichi K., Dijkstra M., Ciardi B., Graziani L.* Ly α -emitting galaxies as a probe of reionization: large-scale bubble morphology and small-scale absorbers // *Mon. Not. Roy. Astron. Soc.* XII 2016. 463. 4019–4040.
- Kanekar N., Wagg J., Chary R. R., Carilli C. L.* A Search for C II 158 μ m Line Emission in HCM 6A, a Ly α Emitter at $z = 6.56$ // *Astrophys. J.* VII 2013. 771. L20.
- Kardashev N. S.* RadioAstron and millimetron space observatories: Multiverse models and the search for life // *Astron. rep.* IV 2017. 61. 310–316.
- Kardashev N. S., Novikov I. D., Lukash V. N., Pilipenko S. V., Mikheeva E. V., Bisikalo D. V., Wiebe D. S., Doroshkevich A. G., Zasov A. V., Zinchenko I. I., Ivanov P. B., Kostenko V. I., Larchenkova T. I., Likhachev S. F., Malov I. F., Malofeev V. M., Pozanenko A. S., Smirnov A. V., Sobolev A. M., Cherepashchuk A. M., Shchekinov Y. A.* Review of scientific topics for the Millimetron space observatory // *Physics Uspekhi*. XII 2014. 57. 1199–1228.
- Kochanek C. S.* The implications of lenses for galaxy structure // *Astrophys. J.* VI 1991. 373. 354–368.
- Koopmans L. V. E.* Gravitational imaging of cold dark matter substructures // *Mon. Not. Roy. Astron. Soc.* Nov 2005. 363, 4. 1136–1144.

- Laporte N., Katz H., Ellis R. S., Lagache G., Bauer F. E., Boone F., Inoue A. K., Hashimoto T., Matsuo H., Mawatari K., Tamura Y.* The absence of [C II] 158 μm emission in spectroscopically confirmed galaxies at $z > 8$ // *Mon. Not. Roy. Astron. Soc.*. VII 2019. 487. L81–L85.
- Larchenkova T. I., Lutovinov A. A., Lyskova N. S.* Modeling the images of relativistic jets lensed by galaxies with different mass surface density distributions // *Astronomy Letters*. IV 2011. 37. 233–247.
- Lynds R., Petrosian V.* Giant Luminous Arcs in Galaxy Clusters // *Bulletin of the American Astronomical Society*. 18. IX 1986. 1014. (BAAS).
- Lyu J., Rieke G. H.* The Intrinsic Far-infrared Continua of Type-1 Quasars // *Astrophys. J.*. VI 2017. 841. 76.
- Mao S., Schneider P.* Evidence for substructure in lens galaxies? // *Mon. Not. Roy. Astron. Soc.*. IV 1998. 295. 587.
- Matthee J., Sobral D., Boogaard L. A., Röttgering H., Vallini L., Ferrara A., Paulino-Afonso A., Boone F., Schaerer D., Mobasher B.* Resolved UV and [C II] Structures of Luminous Galaxies within the Epoch of Reionization // *Astrophys. J.*. VIII 2019. 881. 124.
- Metcalf R. B., Zhao H.* Flux Ratios as a Probe of Dark Substructures in Quadruple-Image Gravitational Lenses // *Astrophys. J.*. III 2002. 567. L5–L8.
- Nayyeri H., Keele M., Cooray A., Riechers D. A., Ivison R. J., Harris A. I., Frayer D. T., Baker A. J., Chapman S. C., Eales S., Farrah D., Fu H., Marchetti L., Marques-Chaves R., Martinez-Navajas P. I., Oliver S. J., Omont A., Perez-Fournon I., Scott D., Vaccari M., Vieira J., Viero M., Wang L., Wardlow J.* Candidate Gravitationally Lensed Dusty Star-forming Galaxies in the Herschel Wide Area Surveys // *Astrophys. J.*. V 2016. 823. 17.
- Negrello M., Hopwood R., De Zotti G., Cooray A., Verma A., Bock J., Frayer D. T., Gurwell M. A., Omont A., Neri R., Dannerbauer H., Leuw L. L., Barton E., Cooke J., Kim S., da Cunha E., Rodighiero G., Cox P., Bonfield D. G., Jarvis M. J., Serjeant S., Ivison R. J., Dye S., Aretxaga I., Hughes D. H., Ibar E., Bertoldi F., Valtchanov I., Eales S., Dunne L., Driver S. P., Auld R., Buttiglione S., Cava A., Grady C. A., Clements D. L., Dariush A., Fritz J., Hill D., Hornbeck J. B., Kelvin L., Lagache G., Lopez-Caniego M., Gonzalez-Nuevo J., Maddox S., Pascale E., Pohlen M., Rigby E. E., Robotham A., Simpson C., Smith D. J. B., Temi P., Thompson M. A., Woodgate B. E., York D. G., Aguirre J. E., Beelen A., Blain A., Baker A. J., Birkinshaw M., Blundell R., Bradford C. M., Burgarella D., Danese L., Dunlop J. S., Fleuren S., Glenn J., Harris A. I., Kamenetzky J., Lupu R. E., Maddalena R. J., Madore B. F., Maloney P. R., Matsuhara H., Michałowski M. J., Murphy E. J., Naylor B. J., Nguyen H., Popescu C., Rawlings S., Rigopoulou D., Scott D., Scott K. S., Seibert M., Smail I., Tuffs R. J., Vieira J. D., van der Werf P. P., Zmuidzinas J.* The Detection of a Population of Submillimeter-Bright, Strongly Lensed Galaxies // *Science*. XI 2010. 330. 800.

- Negrello M., Perrotta F., González-Nuevo J., Silva L., de Zotti G., Granato G. L., Baccigalupi C., Danese L.* Astrophysical and cosmological information from large-scale submillimetre surveys of extragalactic sources // *Mon. Not. Roy. Astron. Soc.*. VI 2007. 377. 1557–1568.
- Paczynski B.* Giant luminous arcs discovered in two clusters of galaxies // *Nature*. II 1987. 325. 572–573.
- Peng C. Y., Impey C. D., Rix H.-W., Kochanek C. S., Keeton C. R., Falco E. E., Lehár J., McLeod B. A.* Probing the Coevolution of Supermassive Black Holes and Galaxies Using Gravitationally Lensed Quasar Hosts // *Astrophys. J.*. X 2006. 649. 616–634.
- Pilipenko S. V., Tkachev M. V., Ermash A. A., Larchenkova T. I., Mikheeva E. V., Lukash V. N.* A model of the cosmic infrared background produced by distant galaxies // *Astronomy Letters*. X 2017. 43. 644–655.
- Planck Collaboration , Aghanim N., Akrami Y., Ashdown M., Aumont J., Baccigalupi C., Ballardini M., Banday A. J., Barreiro R. B., Bartolo N., Basak S., Battye R., Benabed K., Bernard J.-P., Bersanelli M., Bielewicz P., Bock J. J., Bond J. R., Borrill J., Bouchet F. R., Boulanger F., Bucher M., Burigana C., Butler R. C., Calabrese E., Cardoso J.-F., Carron J., Challinor A., Chiang H. C., Chluba J., Colombo L. P. L., Combet C., Contreras D., Crill B. P., Cuttaia F., de Bernardis P., de Zotti G., Delabrouille J., Delouis J.-M., Di Valentino E., Diego J. M., Doré O., Douspis M., Ducout A., Dupac X., Dusini S., Efstathiou G., Elsner F., Enßlin T. A., Eriksen H. K., Fantaye Y., Farhang M., Fergusson J., Fernandez-Cobos R., Finelli F., Forastieri F., Frailis M., Fraisse A. A., Franceschi E., Frolov A., Galeotta S., Galli S., Ganga K., Génova-Santos R. T., Gerbino M., Ghosh T., González-Nuevo J., Górski K. M., Gratton S., Gruppuso A., Gudmundsson J. E., Hamann J., Handley W., Hansen F. K., Herranz D., Hildebrandt S. R., Hivon E., Huang Z., Jaffe A. H., Jones W. C., Karakci A., Keihänen E., Keskitalo R., Kiiveri K., Kim J., Kisner T. S., Knox L., Krachmalnicoff N., Kunz M., Kurki-Suonio H., Lagache G., Lamarre J.-M., Lasenby A., Lattanzi M., Lawrence C. R., Le Jeune M., Lemos P., Lesgourgues J., Levrier F., Lewis A., Liguori M., Lilje P. B., Lilley M., Lindholm V., López-Caniiego M., Lubin P. M., Ma Y.-Z., Macías-Pérez J. F., Maggio G., Maino D., Mandolesi N., Mangilli A., Marcos-Caballero A., Maris M., Martin P. G., Martinelli M., Martínez-González E., Matarrese S., Mauri N., McEwen J. D., Meinhold P. R., Melchiorri A., Mennella A., Migliaccio M., Millea M., Mitra S., Miville-Deschênes M.-A., Molinari D., Montier L., Morgante G., Moss A., Natoli P., Nørgaard-Nielsen H. U., Pagano L., Paoletti D., Partridge B., Patanchon G., Peiris H. V., Perrotta F., Pettorino V., Piacentini F., Polastri L., Polenta G., Puget J.-L., Rachen J. P., Reinecke M., Remazeilles M., Renzi A., Rocha G., Rosset C., Roudier G., Rubiño-Martín J. A., Ruiz-Granados B., Salvati L., Sandri M., Savelainen M., Scott D., Shellard E. P. S., Sirignano C., Sirri G., Spencer L. D., Sunyaev R., Suur-Uski A.-S., Tauber J. A., Tavagnacco D., Tenti M., Toffolatti L., Tomasi M., Trombetti T., Valenziano L., Valiviita J., Van Tent B., Vibert L., Vielva P., Villa F., Vittorio N., Wandelt B. D., Wehus I. K., White M., White S. D. M., Zacchei A., Zonca A.* Planck 2018 results. VI. Cosmological parameters // *arXiv e-prints*. VII 2018. 1807.06209.

- Refsdal S.* On the possibility of determining Hubble’s parameter and the masses of galaxies from the gravitational lens effect // *Mon. Not. Roy. Astron. Soc.*. 1964. 128. 307.
- Riess A. G., Casertano S., Yuan W., Macri L. M., Scolnic D.* Large Magellanic Cloud Cepheid Standards Provide a 1% Foundation for the Determination of the Hubble Constant and Stronger Evidence for Physics beyond Λ CDM // *Astrophys. J.*. V 2019. 876. 85.
- Sanders D. B., Mirabel I. F.* Luminous Infrared Galaxies // *Ann. Rev. Astron. Astrophys.*. 1996. 34. 749.
- Schneider P., Ehlers J., Falco E. E.* Gravitational Lenses. 1992. 112.
- Shibuya T., Ouchi M., Harikane Y., Rauch M., Ono Y., Mukae S., Higuchi R., Kojima T., Yuma S., Lee C.-H., Furusawa H., Konno A., Martin C. L., Shimasaku K., Taniguchi Y., Kobayashi M. A. R., Kajisawa M., Nagao T., Goto T., Kashikawa N., Komiyama Y., Kusakabe H., Momose R., Nakajima K., Tanaka M., Wang S.-Y.* SILVERRUSH. III. Deep optical and near-infrared spectroscopy for Ly α and UV-nebular lines of bright Ly α emitters at $z = 6-7$ // *Publ. Astron. Soc. Japan.* I 2018. 70. S15.
- Silva L., Granato G. L., Bressan A., Danese L.* Modeling the Effects of Dust on Galactic Spectral Energy Distributions from the Ultraviolet to the Millimeter Band // *Astrophys. J.*. XII 1998. 509. 103–117.
- Smirnov A. V., Baryshev A. M., Pilipenko S. V., Myshonkova N. V., Bulanov V. B., Arkhipov M. Y., Vinogradov I. S., Likhachev S. F., Kardashev N. S.* Space mission Millimetron for terahertz astronomy // *Space Telescopes and Instrumentation 2012: Optical, Infrared, and Millimeter Wave.* 8442. IX 2012. 84424C. (Proceedings of the SPIE).
- Soucail G., Fort B., Mellier Y., Picat J. P.* A blue ring-like structure, in the center of the A 370 cluster of galaxies // *Astron. Astrophys.*. I 1987. 172. L14–L16.
- Stark D. P., Richard J., Charlot S., Clément B., Ellis R., Siana B., Robertson B., Schenker M., Gutkin J., Wofford A.* Spectroscopic detections of C III] $\lambda 1909$ Å at $z \sim 6 - 7$: a new probe of early star-forming galaxies and cosmic reionization // *Mon. Not. Roy. Astron. Soc.*. VI 2015. 450. 1846–1855.
- Stark D. P., Richard J., Siana B., Charlot S., Freeman W. R., Gutkin J., Wofford A., Robertson B., Amanullah R., Watson D., Milvang-Jensen B.* Ultraviolet emission lines in young low-mass galaxies at $z \sim 2$: physical properties and implications for studies at $z > 7$ // *Mon. Not. Roy. Astron. Soc.*. XII 2014. 445. 3200–3220.
- Suyu S. H., Bonvin V., Courbin F., Fassnacht C. D., Rusu C. E., Sluse D., Treu T., Wong K. C., Auger M. W., Ding X., Hilbert S., Marshall P. J., Rumbaugh N., Sonnenfeld A., Tewes M., Tikhonova O., Agnello A., Blandford R. D., Chen G. C.-F., Collett T., Koopmans L. V. E., Liao K., Meylan G., Spiniello C.* H0LiCOW - I. H $_0$ Lenses in COSMOGRAIL’s Wellspring: program overview // *Mon. Not. Roy. Astron. Soc.*. VII 2017. 468. 2590–2604.

- Suyu S. H., Treu T., Hilbert S., Sonnenfeld A., Auger M. W., Blandford R. D., Collett T., Courbin F., Fassnacht C. D., Koopmans L. V. E., Marshall P. J., Meylan G., Spiniello C., Tewes M.* Cosmology from Gravitational Lens Time Delays and Planck Data // *Astrophys. J.*. VI 2014. 788. L35.
- Vegetti S., Koopmans L. V. E.* Bayesian strong gravitational-lens modelling on adaptive grids: objective detection of mass substructure in Galaxies // *Mon. Not. Roy. Astron. Soc.*. Jan 2009. 392, 3. 945–963.
- Vieira J. D., Marrone D. P., Chapman S. C., De Breuck C., Hezaveh Y. D., Weiß A., Aguirre J. E., Aird K. A., Aravena M., Ashby M. L. N., Bayliss M., Benson B. A., Biggs A. D., Bleem L. E., Bock J. J., Bothwell M., Bradford C. M., Brodwin M., Carlstrom J. E., Chang C. L., Crawford T. M., Crites A. T., de Haan T., Dobbs M. A., Fomalont E. B., Fassnacht C. D., George E. M., Gladders M. D., Gonzalez A. H., Greve T. R., Gullberg B., Halverson N. W., High F. W., Holder G. P., Holzappel W. L., Hoover S., Hrubes J. D., Hunter T. R., Keisler R., Lee A. T., Leitch E. M., Lueker M., Luong-van D., Malkan M., McIntyre V., McMahon J. J., Mehl J., Menten K. M., Meyer S. S., Mocuano L. M., Murphy E. J., Natoli T., Padin S., Plagge T., Reichardt C. L., Rest A., Ruel J., Ruhl J. E., Sharon K., Schaffer K. K., Shaw L., Shirokoff E., Spilker J. S., Stalder B., Staniszewski Z., Stark A. A., Story K., Vanderlinde K., Welikala N., Williamson R.* Dusty starburst galaxies in the early Universe as revealed by gravitational lensing // *Nature*. III 2013. 495. 344–347.
- Walsh D., Carswell R. F., Weymann R. J.* 0957 + 561 A, B - Twin quasistellar objects or gravitational lens // *Nature*. V 1979. 279. 381–384.
- Weisz D. R., Dolphin A. E., Skillman E. D., Holtzman J., Gilbert K. M., Dalcanton J. J., Williams B. F.* The Star Formation Histories of Local Group Dwarf Galaxies. II. Searching For Signatures of Reionization // *Astrophys. J.*. VII 2014. 789. 148.
- Wong K. C., Suyu S. H., Chen G. C.-F., Rusu C. E., Millon M., Sluse D., Bonvin V., Fassnacht C. D., Taubenberger S., Auger M. W., Birrer S., Chan J. H. H., Courbin F., Hilbert S., Tikhonova O., Treu T., Agnello A., Ding X., Jee I., Komatsu E., Shajib A. J., Sonnenfeld A., Blandford R. D., Koopmans L. V. E., Marshall P. J., Meylan G.* H0LiCOW XIII. A 2.4% measurement of H_0 from lensed quasars: 5.3σ tension between early and late-Universe probes // *arXiv e-prints*. VII 2019. 1907.04869.
- Xu D., Sluse D., Gao L., Wang J., Frenk C., Mao S., Schneider P., Springel V.* How well can cold dark matter substructures account for the observed radio flux-ratio anomalies // *Mon. Not. Roy. Astron. Soc.*. III 2015. 447. 3189–3206.
- Xu D. D., Mao S., Wang J., Springel V., Gao L., White S. D. M., Frenk C. S., Jenkins A., Li G., Navarro J. F.* Effects of dark matter substructures on gravitational lensing: results from the Aquarius simulations // *Mon. Not. Roy. Astron. Soc.*. IX 2009. 398. 1235–1253.

Zemcov M., Blain A., Cooray A., Béthermin M., Bock J., Clements D. L., Conley A., Conversi L., Dowell C. D., Farrah D., Glenn J., Griffin M., Halpern M., Jullo E., Kneib J.-P., Marsden G., Nguyen H. T., Oliver S. J., Richard J., Roseboom I. G., Schulz B., Scott D., Shupe D. L., Smith A. J., Valtchanov I., Viero M., Wang L., Wardlow J. HerMES: A Deficit in the Surface Brightness of the Cosmic Infrared Background due to Galaxy Cluster Gravitational Lensing // *Astrophys. J.*. VI 2013. 769. L31.